# Optimal Operation of Smart Buildings with Stochastic Connection of Electric Vehicles

Jiachang Huang
*School of Automation*
*Guangdong University of Technology*
Guangzhou, China
hjiachang@foxmail.com

Dongxiao Wang
*School of Automation*
*Guangdong University of Technology*
Guangzhou, China
dongxiaouon@gmail.com

Runji Wu
*School of Automation*
*Guangdong University of Technology*
Guangzhou, China
runjiwu@foxmail.com

Chun Sing Lai
*School of Automation*
*Guangdong University of Technology*
Guangzhou, China
chunsing.lai@brunel.ac.uk

Changhong Xie
*School of Automation*
*Guangdong University of Technology*
Guangzhou, China
2111904168@mail2.gdut.edu.cn

Zhuoli Zhao
*School of Automation*
*Guangdong University of Technology*
Guangzhou, China
zhuoliscut@gmail.com

Loi Lei Lai
*School of Automation*
*Guangdong University of Technology*
Guangzhou, China
l.l.lai@gdut.edu.cn

*Abstract*—One of the key domains in smart cities is smart energy in which smart grid is a main focus. In recent years, with the development of smart grid, controllable air conditioning load participating in demand response projects and the application of renewable energy sources have drawn wide research interests. The integration of photovoltaic (PV) system and electric vehicles into the micro grid has also brought vitality to the stable operation of smart grids. In this paper, a novel control scheme is proposed to optimize the scheduling of building micro grid that integrate controllable air conditioner loads, PV panels and electric vehicles. The optimal operation problem is modeled and further converted into a mixed integer linear programming (MILP) problem whose objective function is minimizing the electricity cost of the building. The stochastic characteristics of electric vehicles are also considered in this paper to better model electric vehicle behaviors. Simulations are conducted on an office building micro grid and the simulation results verify the feasibility of proposed control strategy.

*Keywords—Air conditioner resources, building micro grid, electric vehicles, stochastic characteristics*

## Nomenclature

### Abbreviations

| | |
|---|---|
| EVs | Electric vehicles |
| ACLs | Air conditioner loads |
| DR | Demand response |
| PV | Photovoltaic |
| SoC | State of charge |
| MILP | Mixed integer linear programming |

### Indices

| | |
|---|---|
| $t$ | Index of time interval ($t = 1,2,\ldots,N$) |
| $i$ | Index for electric vehicles ($i= 1,2,\ldots,I$) |
| $N$ | Number of time intervals for the scheduling time horizon |
| $I$ | Number of EVs considered |

### Parameters

| | |
|---|---|
| $C_{pa}$ | Air heat capacity [J/kg/$^\circ$C] |
| $C_{pw}$ | Wall heat capacity [J/kg/$^\circ$C] |
| $E_{EV,i}$ | Rated capacity of the i-th EV [kWh] |
| $G_{std}$ | Solar radiation intensity in the standard situation [W/m$^2$] |
| $M_a$ | Air mass [kg] |
| $M_w$ | Wall mass [kg] |
| $P_{EV,i}^{\max}$ | Maximum battery charging/discharging power of the i-th electric vehicle [kW] |
| $P_{grid}^{\max}$ | Maximum power exchanged with the external grid [kW] |
| $P_{PV,rated}$ | Rated output power of photovoltaic panels [kW] |
| $R_C$ | A certain radiation intensity point, set to be 200W/m$^2$ |
| $R_{eq}$ | Equivalent thermal resistance of the building envelope |
| $R_{wa}$ | Equivalent thermal resistance between the exterior surface of the building wall and the external environment |
| $R_{wr}$ | Equivalent thermal resistance between the interior surface of the building wall and the interior air of the building |
| $SoC_{EV,i,init}$ | Initial SoC of the i-th EV [%] |
| $SoC_{EV,i,dep}$ | SoC of the i-th EV when departing [%] |
| $SoC_{EV}^{\min}$ $SoC_{EV}^{\max}$ | Minimum and maximum SoC of the electric vehicle [%] |
| $t_{arr,i}$ | Arrival time to the building of the i-th EV |
| $t_{dep,i}$ | Departure time from the building of the i-th EV |
| $T_a^{\min}$ $T_a^{\max}$ | Minimum and maximum required value of the air temperature within |

| | |
|---|---|
| | building [ °C ] |
| $T_w^{\min}$  $T_w^{\max}$ | Minimum and maximum required value of the building wall [ °C ] |
| $\eta_{EV,i}$ | Charging/discharging efficiency of the i-th EV [%] |
| $\tau$ | Length of each time interval [h] |

### *Variables*

| | |
|---|---|
| $C_{buy}(t)$ | The retail electricity price of grid at time interval t [RMB/kWh] |
| $C_{sell}(t)$ | PV feed-In tariff at time interval t [RMB/kWh] |
| $G(t)$ | Solar radiation intensity forecast at time interval t [W/m$^2$] |
| $P_{ac}(t)$ | Air conditioner actual power at time interval t [kW] |
| $P_{EV,i,ch}(t)$ | Charging power of the i-th EV at time interval t [kW] |
| $P_{EV,i,dch}(t)$ | Discharging power of the i-th EV at time interval t [kW] |
| $P_{grid,buy}(t)$ | Power bought from external grid at time interval t [kW] |
| $P_{grid,sell}(t)$ | Power sold to external grid at time interval t [kW] |
| $P_{LD,basic}(t)$ | Basic load power at time interval t [kW] |
| $P_{PV}(t)$ | PV panel output power at time interval t [kW] |
| $Q_{ac}(t)$ | Cooling/heating capacity of air conditioning at time interval t [J] |
| $S_{ac}(t)$ | Operation state of air conditioners at time interval t |
| $SoC_{EV,i}(t)$ | SoC of the i-th EV at time interval t [%] |
| $T_{amb}(t)$ | Ambient temperature at time interval t [ °C ] |
| $T_a(t)$ | Air temperature inside the building at time interval t [ °C ] |
| $T_w(t)$ | Wall temperature of the building at time interval t [ °C ] |

## I INTRODUCTION

In the context of smart cities, buildings are playing a more and more crucial part in the distribution network operation due to its high electricity consumption. According to [1], buildings represent for more than 50% of the global electricity consumption, and among the electricity consumed by buildings, about 32% comes from air conditioner loads (ACLs), especially in the hot summer day. Besides, the ACLs can also participate in demand response (DR) projects due to their heat storage buffers [2], which means that buildings can reduce their electricity costs by the directly control of ACLs.

At present, a lot of research has been done on the participation of ACLs in DR projects. In [3], a residential inverter air conditioning model which is based on DR control scheme is proposed to realize the automatic and optimal response to day-ahead electricity price. In [4], a hierarchical scheduling strategy for multiple groups of virtual energy storage systems is proposed with the aim to adjust the voltage of the low-voltage grid while meeting the thermal comfort of users.

In addition, because of the progress of smart grid, distributed renewable energy resources have been gradually applied in buildings, especially solar photovoltaic (PV) panels, which are widely installed in residential or commercial buildings [5]. Electric vehicles, as an effective solution to deal with the issues caused by fossil fuel usage and reduce greenhouse gas emissions, have been widely promoted in recent years [6]. In the development of a smart city, a building micro grid consisting of electrical vehicles (EVs) and solar photovoltaic system may have an important effect on reducing building electricity consumption and alleviating power grid pressure.

Researchers have made great effort to the charging strategies of EVs in the buildings including both EVs and PV system. In [7], based on the prediction of photovoltaic output, with the objective of determining the optimal charging plan for electric vehicles, a charging scheme for intelligent electric vehicles for smart houses/buildings with photovoltaic systems is proposed. In [8], with the aim of reducing the daily electricity cost of plug-in hybrid electric vehicles (PHEVs) and ease the impact caused by charging parks on the main power grid, a real time energy control scheme of charging parks in industrial or commercial offices is proposed.

As far as the existing literature is concerned, most of the current research is devoted to the charging strategies for electric vehicles under the interaction of EV and PV system without considering the optimal control of air conditioning resources. Few of them try to build a precise air conditioner control model to coordinate the intermittency of photovoltaic power generation. In addition, there are few researches on the bidirectional energy exchange between electric vehicles and building for the building micro grid containing photovoltaic systems and electric vehicles. To address the research gap, this paper proposes a novel building micro grid scheduling strategy to integrate the building's air conditioning loads, photovoltaic system and electric vehicles. Considering the bidirectional energy exchange between electric vehicles and building micro grid, a coordinated control strategy is proposed to reduce the electricity cost of the building. The control strategy is further converted into an MILP problem.

The remaining parts of the paper is presented as follows. The proposed building micro grid is introduced in Section II. Section III presents the components modeling. Section IV analyzes the case study and the simulation results. The conclusion is drawn in Section V.

## II SMART BUILDING MICROGRID

In this section, the components and structure of an office building micro grid are given, which are shown in Fig. 1. As can be seen, the components include a series of PV panels, basic loads and controllable ACLs of the building and some EVs. The electricity generated by the PV panels is consumed by the building's load, with the rest is used to charge electric vehicles. The air conditioner loads, as the controllable loads in

the building, are directly controlled by ACLs controller. Through the EVs controller, all electric vehicles connected to the system can exchange energy with the building in a bidirectional way. In addition, the stochastic characteristics of electric vehicles are modeled in this paper, so as to better capture the operation scenario. More details about the office building micro grid are given in the Case Study section.
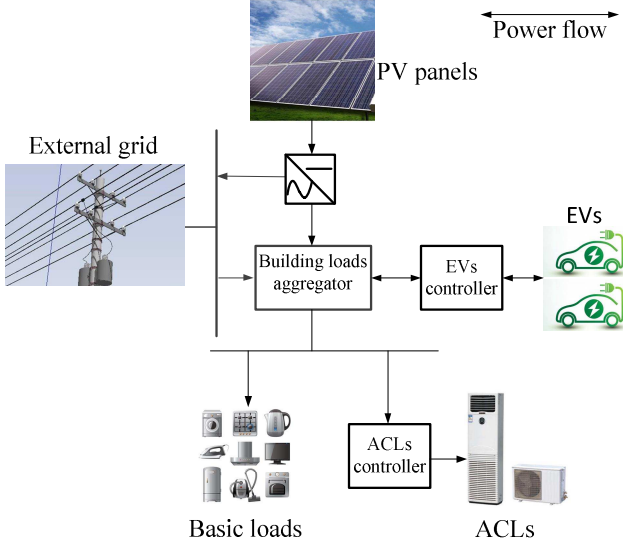


Fig. 1. Components and configuration of the proposed building microgrid.

## III COMPONENT MODELLING

The entire scheduling cycle (24 hours) is divided into N time intervals t. It is assumed that within each time interval t, the values of all status variables in the system remain constant. N is set to be 96 and t is 15 minutes in this paper.

### A. Photovoltaic Panels

The output power of photovoltaic panels depends on the intensity of solar radiation. According to [9], when the solar radiation intensity falls below a definite value, the PV panels' output power is positively correlated to the square value of the solar radiation intensity. Vice versa, the output power is positively correlated to the solar radiation intensity. The PV panels' output power model can be described as follows:

$$P_{PV}(t) = \begin{cases} P_{PV,rated}(\dfrac{G(t)}{G_{std}R_C})^2, & for\ 0 \le G(t) < R_C \\ P_{PV,rated}\dfrac{G(t)}{G_{std}}, & for\ G(t) \ge R_C \end{cases} \quad (1)$$

### B. Air Conditioner Loads

In order to control the air conditioning load as a demand response resource optimally while meeting the indoor temperature requirements of the occupants, the thermodynamic process inside the building needs to be analyzed. As shown in Fig. 2(a), the widely used one-parameter model, which only considers the thermal resistance of the wall and considers that the heat swap between the building internal air and external environment[10]. In this work, a more exact two-parameter model as shown in Fig. 2(b) is adopted, which takes the heat swap between the wall and the inside/outside of the building

into account on the premise of considering the heat swap between the building's internal space and the external ambient [11].
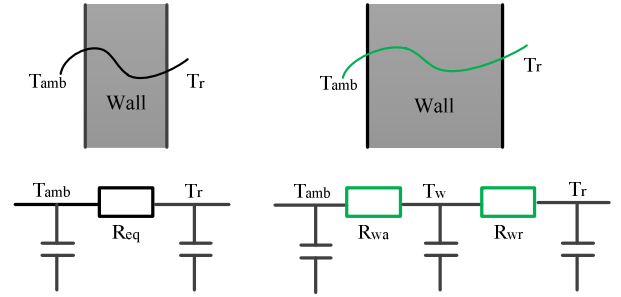


Fig. 2. Dynamic thermal model: (a) one-parameter model (b) two-parameter model.

According to [12], the two-parameter dynamic thermal model is described as follows:

$$T_a(t) = (1 - \frac{1}{M_a C_{pa} R_{eq}})T_a(t-1) + \frac{1}{M_a C_{pa} R_{eq}}T_{amb}(t-1)$$
$$+ \frac{T_w(t-1) - T_a(t-1)}{M_a C_{pa} R_{wr}} - S_{ac}(t-1)\frac{Q_{ac}(t-1)}{M_a C_{pa}}, \forall t \in [1, N] \quad (2)$$

$$T_w(t) = T_w(t-1) + \frac{T_{amb}(t-1) - T_w(t-1)}{M_w C_{pw} R_{wa}} + \frac{T_a(t-1)}{M_w C_{pw} R_{wr}}$$
$$- \frac{T_w(t-1)}{M_w C_{pw} R_{wr}}, \forall t \in [1, N] \quad (3)$$

$$Q_{ac}(t) = P_{ac}(t) \cdot COP \cdot \tau \quad (4)$$

### C. Electric Vehicle

#### a. Stochastic Characteristics

In this paper, to better simulate the actual daily behavior of electric vehicles, the stochastic characteristic distribution of 20 electric vehicles is analyzed and generated, including the time of reaching the office building and the detention time of staying in the office building. On the one hand, according to [13], the arrival time of each electric vehicle can be described by chi-square distribution, and the corresponding probability density distribution function is shown below:

$$f(x) = \frac{x^{(n-2)/2}}{2^{n/2} \cdot \Gamma(n/2)} \cdot e^{-x/2} \quad (5)$$

Herein, $\Gamma(\bullet)$ is defined as $\Gamma(a) = \int_0^\infty x^{a-1} \cdot e\ dx, a > 0$, $x$ refers to the arrival time of each EV and the freedom degrees n is set to be 4. The distribution graph of generated different arrival time of the EVs is shown in Fig. 3. It can be found that most of the EVs arrive in the office building in the morning, which is consistent with people's work habits.
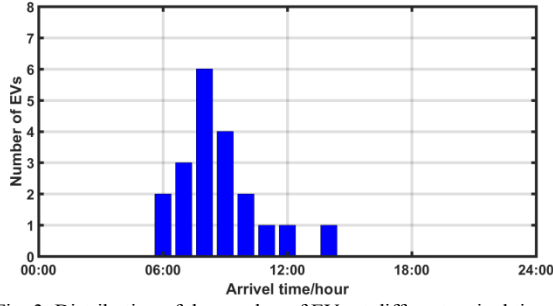
Fig. 3. Distribution of the number of EVs at different arrival time.

On the other hand, the detention time of EVs staying in the building is assumed to conform to the normal distribution [14] whose mean value is set as 10 hours and variance is set as 1 hour. The distribution graph of generated different detention time of the EVs is given in Fig. 4. In addition, the incipient SoC of each EV's battery can be expressed by the uniform distribution between 0.4 and 0.8, and in this paper, the incipient SoC of each EV is generated through the Monte Carlo simulation.
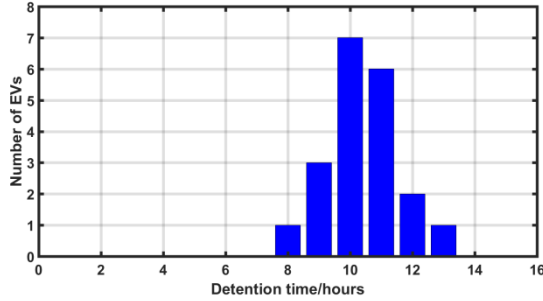

Fig. 4. Distribution of the number of EVs with different detention time.

### b. Charging/discharging Model

According to [15], considering the SoC limit and charging/discharging power limits of each EV, the charging/discharging process of the battery for the i-th EV can be described as follows:

$$SoC_{EV,i}(t) = \frac{P_{EV,i,ch}(t-1) - P_{EV,i,dch}(t-1)}{E_{EV,i}} \cdot \eta_{EV,i} \cdot \tau$$
$$+ SoC_{EV,i}(t-1), \forall i \in I, t \in (t_{arr,i}, t_{dep,i}] \tag{6}$$

$$SoC_{EV,i}(t) = SoC_{EV,i,init}, \forall i \in I, t = t_{arr,i} \tag{7}$$

$$SoC_{EV,i} = SoC_{EV,i,dep}, \forall i \in I, t = t_{dep,i} \tag{8}$$

$$SoC_{EV}^{min} \le SoC_{EV,i}(t) \le SoC_{EV}^{max}, \forall i \in I, t \in [t_{arr,i}, t_{dep,i}] \tag{9}$$

$$0 \le P_{EV,i,ch}(t), P_{EV,i,dch}(t) \le P_{EV,i}^{max}, \forall i \in I, t \in [t_{arr,i}, t_{dep,i}] \tag{10}$$

Constrains (7) and (8) define the SoC values of the EV's battery the moments of arrival and departure. Constraint (9) ensures that the battery of every electric vehicle will not be overcharged or over-discharged. For simplicity, the maximum SoC value and minimum SoC value of each EV in this paper are set as 90% and 20% respectively.

### D. Objective Function

The aim of the building micro grid is to minimize the total daily electricity cost of the building under the premise of meeting the relevant constraints. In addition, the electricity cost of the building relies not only on the electricity amount swap between the building and power grid, but also on the price of electricity. Therefore, in this paper, the objective function is shown in Equation (11), with the goal being to minimize the total electricity cost of the building micro grid in the whole operating period.

$$\min \sum_{t=1}^{N} [P_{grid,buy}(t) \cdot C_{buy}(t) - P_{grid,sell}(t) \cdot C_{sell}(t)] \cdot \tau \tag{11}$$

### E. Related Constraints

To maintain the stable operation of the building micro grid, load balancing constraints and system operation constraints need to be met. The specific constraints to be met are as follows:

### a. Temperature Comfort Constraints

Ensuring the temperature comfort of the occupants in the building is the fundamental requirement of air conditioning building participating in demand response scheme. The indoor temperature comfort constraint is shown in Constraint (12), and the wall temperature comfort constraint is expressed in Constraint (13). In addition, the air conditioners' operation status is expressed by a binary integer variable $S_{ac}(t)$, as shown in Constraint (14), where $S_{ac}(t) = 1$ means the air conditioners are ON while $S_{ac}(t) = 0$ means the air conditioners are OFF.

$$T_r^{min} \le T_r(t) \le T_r^{max}, \forall t \in [1, N] \tag{12}$$

$$T_w^{min} \le T_w(t) \le T_w^{max}, \forall t \in [1, N] \tag{13}$$

$$S_{ac}(t) = \begin{cases} 1, & ON \\ 0, & OFF \end{cases} \tag{14}$$

### b. Power Balance Constraints

In the stable operation state, the input power of the building micro grid should be balanced with the consumed power at each moment. In the meantime, the exchanged electricity amount between the building micro grid and the external distribution network cannot more than the maximum capacity of the transmission line. The constraints mentioned above are described as follows:

$$P_{PV}(t) + P_{grid,buy}(t) + \sum P_{EV,i,dch}(t) - \sum P_{EV,j,ch}(t)$$
$$= P_{ac}(t) \cdot S_{ac}(t) + P_{LD,basic}(t) + P_{grid,sell}(t), \forall t \in [1, N] \tag{15}$$

$$0 \le P_{grid,buy}(t), P_{grid,sell}(t) \le P_{grid}^{max}, \forall t \in [1, N] \tag{16}$$

### IV CASE STUDY

In this paper, an office building, equipped with 50 rooms and air conditioners in Fudian Data Center in Foshan city, Guangdong Province, is selected as the research object for experimental simulation.

## A    Simulation setup

The components and structure of the building is shown in Fig. 1 in Section II. The PV panels' rated output power is set as 200kW in this test system. The relevant parameters of each EVs battery, such as battery capacity, charge/discharge power and charge/discharge efficiency, are 24kWh, 7.68kW and 90%, respectively [16]. In addition, the SoC value of each electric vehicle's battery when leaving is set to be equal to that when it arrives. The system model is implemented in MATLAB and solved by Mosek toolbox [17].

For simplicity, this paper assumes that all rooms in the simulated building have the standard size and the same thermal comfort range, and the room parameters and indoor temperature comfort ranges are shown in Table.1. In addition, the rated power of air conditioners is set to be 3kW. As for other experimental data, the ambient temperature data is available from China Meteorological website [18], while the data of electricity prices can be obtain from China Southern Power Grid [19]. The ambient temperature and electricity prices of a summer day in Foshan city are shown in Fig. 5. As seen in Fig. 5, the peak ambient temperature time is between about 13:00 to 16:00, while the peak electricity price time appears between 10:00 to 13:00 and 18:00 to 21:00.

Table.1.Building' parameter ranges.

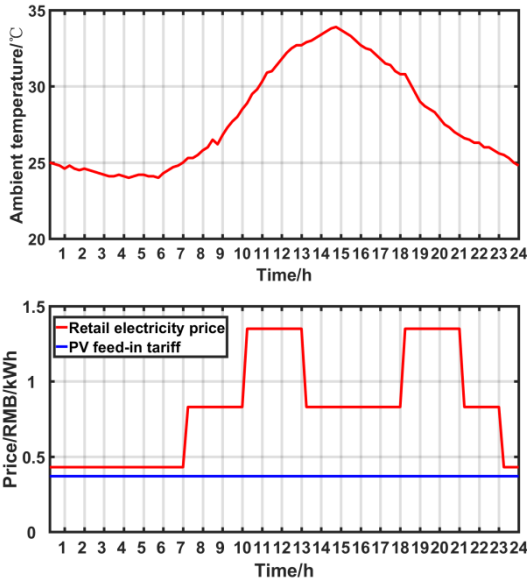| Rooms' length/ width/ height/m | Wall's thickness / m | $T_a^{min}$ / °C | $T_a^{max}$ / °C |
|---|---|---|---|
| 16/12/3.5 | 0.3 | 23 | 27 |



Fig. 5. (a) Ambient temperature (b) Day-ahead electricity prices.

## B    Simulation Results and analysis

The operation status of air conditioners and the indoor air temperature changes of the office building in a day are shown in Fig. 6 and Fig. 7, respectively. As can be seen from Fig. 6, the air conditioner is turned on before the peak electricity price comes to pre-cool the indoor air temperature of the building, and it is turned off at certain times during the peak electricity price period. This action can help reducing the operating cost of the building while ensuring the user's thermal comfort. As shown in Fig. 7, the temperature inside the building is well controlled within the set thermal comfort range.
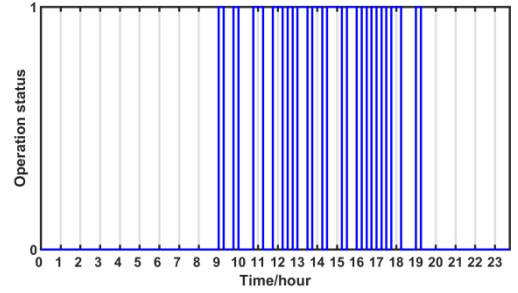


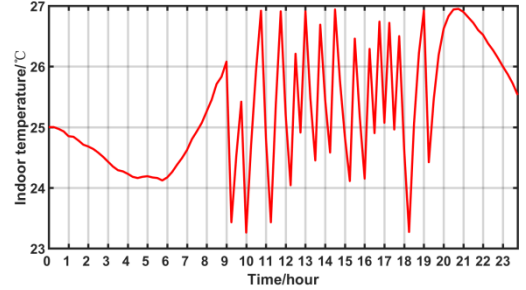Fig. 6. ACs operation status in the office building in a day.



Fig. 7. Air temperature changes in the office building in a day.

The SoC changes for the batteries of EV1 to EV20 are indicated in Fig. 8 to Fig. 11. It is worth mentioning that the SoC record of each EV's battery by the building micro grid begins when the EV arrives at the building and ends when the EV leaves. Therefore, the time corresponding to the starting point of the battery SoC change curve of each EV is its arrival time, while the time corresponding to the end point is its departure time. As can be seen, during the two electricity price peak time periods (10:00 to 13:00, and 18:00 to 21:00), the SoC curves of all electric vehicle batteries are basically a downward trend, which means that during these two time periods, electric vehicles are discharging for meeting the building load consumption to reduce the building's electricity purchase from the external grid.
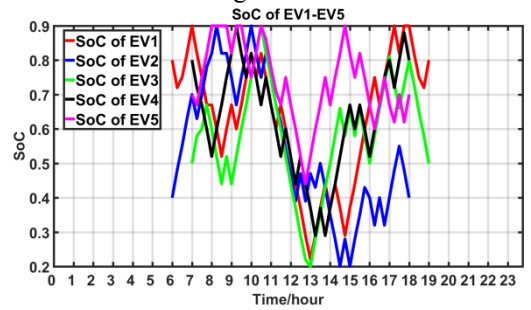


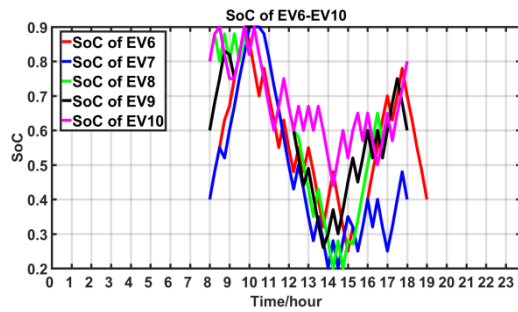Fig. 8. SoC changes of the batteries of EV1 to EV5.

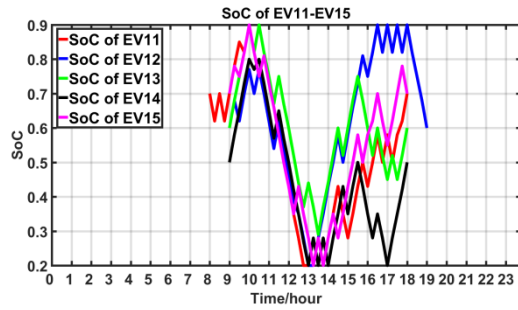Fig. 9. SoC changes of the batteries of EV6 to EV10.



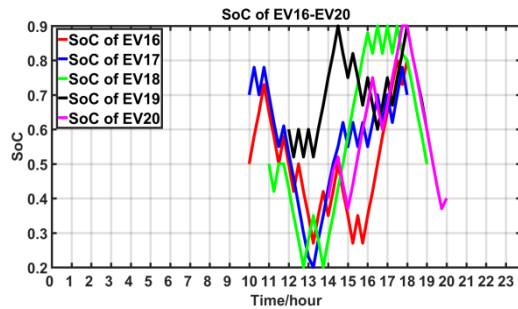Fig. 10. SoC changes of the batteries of EV11 to EV15.



Fig. 11. SoC changes of the batteries of EV16 to EV20.

The amount of power exchanged between the building and the distribution grid is demonstrated in Fig. 12. The positive value indicates that the building buys electricity from the external grid. It can be observed that during peak electricity prices (mainly during 10:00-13:00), due to the discharging behavior of electric vehicles, the amount of power purchased by the building from the distribution grid is greatly reduced.
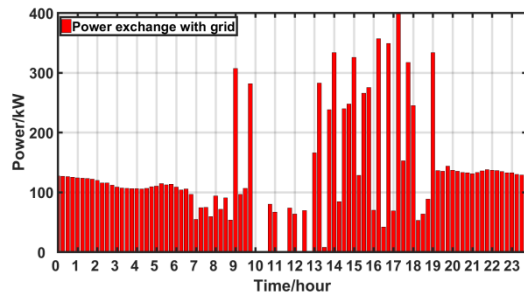


Fig. 12. Power exchange with grid.

In order to prove that the proposed building micro grid can indeed reduce the electricity cost of building, this paper compares the system operating cost with the case where all the electricity required is purchased from the distribution grid. By connecting photovoltaic power panels and electric vehicles to the building micro grid, the system's operating cost in one day is 2515 RMB. Correspondingly, without photovoltaic panels and electric vehicles, the electricity cost of the system for a day is 4513 RMB. Therefore, to some extent, the building micro grid and its control strategy proposed in this paper can reduce the electricity cost of building.

## V    CONCLUSION

This work presents a novel building microgrid containing PV panels, building loads (controllable AC loads and uncontrollable loads) and electric vehicles. The optimal scheduling problem of the building micro grid is converted into a mixed integer linear programming (MILP) problem, with the objective of reducing the electricity cost of the building on the condition of ensuring the indoor temperature comfort of end-users and the interests of EV owners. The simulation is conducted on an office building in the Foshan Data Center, The simulation results show that this proposed strategy can reduce the electricity cost of building by reducing the amount of electricity purchased during the peak load of the power grid.

REFERENCES

[1] Yoon A, Kim Y, Zakula T, and Moon S, "Retail electricity pricing via online-learning of data-driven demand response of HVAC systems," *Applied Energy*, vol.265, 2020.

[2] Wang Q, Liao J, Su Y, et al, "An optimal reactive power control method for distribution network with soft normally-open points and controlled air-conditioning loads," *International Journal of Electrical Power & Energy Systems*, vol.103, pp. 421-430, 2018.

[3] Hu M, and Xiao F, "Price-responsive model-based optimal demand response control of inverter air conditioners using genetic algorithm," *Applied Energy*, vol.219, pp. 151-164, 2018.

[4] Wang D, Meng K, Gao X, et al, "Coordinated dispatch of virtual energy storage systems in LV grids for voltage regulation," *IEEE Transactions on Industrial Informatics*, vol.14, pp. 2452-2462, 2018.

[5] Zhang S, Huang P, and Sun Y, "A multi-criterion renewable energy system design optimization for net zero energy buildings under uncertainties," *Energy*, vol.94, pp. 654-665, 2016.

[6] Parinaz A, Mohammadiivatloo B, and Abapour M, "Risk-based scheduling strategy for electric vehicle aggregator using hybrid

Stochastic/IGDT approach," *Journal of Cleaner Production*, vol.248, 2020.

[7] Wi Y, Lee J, and Joo S, "Electric vehicle charging method for smart homes/buildings with a photovoltaic system," *IEEE Transactions on Consumer Electronics*, vol.59, pp. 323-328, 2013.

[8] Mohamed A, Salehi V, Ma T, and Mohammed O A, "Real-time energy management algorithm for plug-in hybrid electric vehicle charging parks involving sustainable energy," *IEEE Transactions on Sustainable Energy*, vol.5, pp. 577-586, 2014.

[9] Reddy S S, Bijwe P R, and Abhyankar A R, "Real-time economic dispatch considering renewable power generation variability and uncertainty over scheduling period," *IEEE Systems Journal*, vol. 9, pp. 1440-1451, 2015.

[10] Massouros P, Athanassouli G, and Massouros G, "A model of the thermal transient state of a wall of a room during the heating by a heating system," *International Journal of Energy Research*, vol. 24, pp. 779-789, 2000.

[11] Bălan R, Cooper J, Chao K, Stan S, and Donca R, "Parameter identification and model based predictive control of temperature inside a house," *Energy and Buildings*, vol. 43, pp. 748-758, 2011.

[12] Wang D, Meng K, Gao X, Coates C, and Dong Z Y, "Optimal air-conditioning load control in distribution network with intermittent renewables," *Journal of Modern Power Systems and Clean Energy*, vol. 5, pp. 55-65, 2017.

[13] Wang D, Guan X, Wu J, et al, "Integrated energy exchange scheduling for multimicrogrid system with electric vehicles," *IEEE Transactions on Smart Grid*, vol. 7, pp. 1762-1774, 2016.

[14] Jian L, Zheng Y, Xiao X, and Chan C C, "Optimal scheduling for vehicle-to-grid operation with stochastic connection of plug-in electric vehicles to smart grid," *Applied Energy*, vol. 146, pp. 150-161, 2015.

[15] Thomas D, Deblecker O, and Ioakimidis C S, "Optimal operation of an energy management system for a grid-connected smart building considering photovoltaics' uncertainty and stochastic electric vehicles' driving schedule," *Applied Energy*, vol. 210, pp. 1188-1206, 2018.

[16] Nissan, Nissan Leaf Specifications onlines; 2020. Available: https://www.nissan.co.uk/vehicles/new-vehicles/leaf.html

[17] MOSEK. The MOSEK optimization toolbox for MATLAB manual. Version 9.2. Available. https://docs.mosek.com/9.2/toolbox/index.html. Accessed 23/6/2020.

[18] China Meteorological Data Website. Available: http://data.cma.cn/ (Visited on 5 July 2020).

[19] China Southern Power Grid. Available: http://www.csg.cn/(Visited on 5 July 2020).